

Sinking of a Horizontal Cylinder

Dominic Vella

*Institute of Theoretical Geophysics, Department of Applied Mathematics and Theoretical Physics,
University of Cambridge, Wilberforce Road, CB3 0WA United Kingdom*

Duck-Gyu Lee and Ho-Young Kim*

School of Mechanical and Aerospace Engineering, Seoul National University, Seoul 151-744, Korea

Received December 8, 2005. In Final Form: February 17, 2006

We study the sinking of a dense cylinder initially supported horizontally at an air–water interface and then released. The sinking motion is studied experimentally and agrees quantitatively with a simple hydrodynamic model of the process. In particular, our model predicts that the time taken for the cylinder to become immersed in the liquid should be $t_{\text{sink}} \sim \mathcal{O}((l_c/g)^{1/2})$, where l_c is the capillary length and g the acceleration due to gravity, in good agreement with what is observed experimentally.

It is well-known that the tension of the interface between a liquid and a gas may allow sufficiently small objects to remain afloat at the interface even if their density is substantially larger than that of the liquid. Although this effect is a matter of life and death for water-walking creatures who rely on it to avoid drowning,^{1–3} it is also of importance in practical situations such as mineral flotation as well as the emerging field of self-assembly using capillary forces.⁴

Although some attention has been given to understanding when objects can float in equilibrium at an interface,^{2,5,6} the question of how an object sinks if the balance of forces is upset has not been considered. This can happen if the vertical force that surface tension provides is reduced suddenly, which is most easily achieved by adding surfactant to the water. Contact between two objects can also lead to sinking, however, because a portion of the meniscus is then eliminated.⁷ To highlight the important aspects of this dynamic process, we study here a simple system that is amenable to both experimental and theoretical investigation and find good agreement between the two approaches.

In a typical experiment, a circular cylinder lies horizontally at the interface between a liquid and a gas, as shown in Figure 1. The density, ρ_s , of the cylinder is chosen such that the interfacial tension, γ , and the weight of displaced fluid (of density ρ) are too small for the cylinder to remain afloat without some external support. Once this support is removed, the cylinder sinks rapidly taking $\mathcal{O}(0.1)$ s to become completely immersed in the bulk fluid. The dynamics of the sinking process are illustrated by the time series in Figure 2.

To determine the subsequent motion of the cylinder, we develop a simple hydrodynamic model of the motion allowing us to predict the height, h_0 , of the cylinder's center above the undeformed free surface as a function of time t after release. Rather than adopt a purely numerical strategy such as that of Gaudet,⁸ we assume

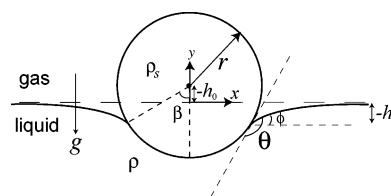


Figure 1. Geometry of a cylinder lying horizontally at the interface between a liquid and a gas.

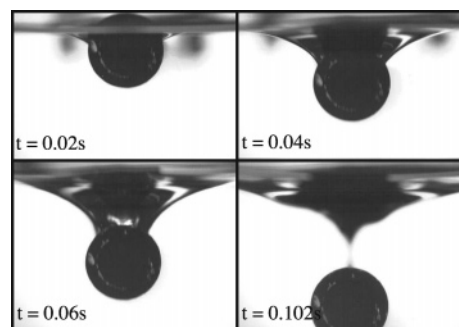


Figure 2. Time series of the sinking motion for a cylinder of diameter 5.09 mm (i.e., $R = 0.93$) with $\rho_s = 1920 \text{ kg m}^{-3}$ (i.e., $\mathcal{D} = 1.92$) viewed along its axis through the wall of a transparent tank.

that the meniscus surrounding the cylinder remains in hydrostatic equilibrium, an assumption that we expect to be valid for times that are short compared to the characteristic time $t_c \equiv (\gamma/\rho g^3)^{1/4}$, where g is the acceleration due to gravity. This characteristic time is that taken for capillary gravity waves to travel the capillary length, $l_c \equiv (\gamma/\rho g)^{1/2}$, and provides a convenient nondimensionalisation of time. Similarly, l_c and γ are the natural scales for all lengths and forces per unit length, respectively. We adopt these nondimensionalisations henceforth and denote nondimensional quantities by uppercase letters.

In the experiments we performed (described below), the Reynolds number of the motion was typically 250. We therefore assume that the flow induced in the liquid by sinking is potential flow so that the velocity field in the fluid may be written $\mathbf{u} = \nabla\varphi$, where $\nabla^2\varphi = 0$. This problem is considered in many elementary texts on fluid mechanics^{9,10} for a cylinder of infinite

(9) Acheson, D. J. *Elementary Fluid Dynamics*; Oxford University Press: Oxford, 1990.

* Corresponding author.

- (1) Bush, J. W. M.; Hu, D. L. *Annu. Rev. Fluid Mech.* **2006**, *38*, 339–369.
- (2) Gao, X.; Jiang, L. *Nature* **2004**, *432*, 36.
- (3) Hu, D. L.; Chan, B.; Bush, J. W. M. *Nature* **2003**, *424*, 663–666.
- (4) Whitesides, G. M.; Grzybowski, B. *Science* **2002**, *295*, 2418–2421.
- (5) Rapacchietta, A. V.; Neumann, A. W. *J. Colloid Interface Sci.* **1977**, *59*, 555–567.
- (6) Rapacchietta, A. V.; Neumann, A. W.; Omenyi, S. N. *J. Colloid Interface Sci.* **1977**, *59*, 541–554.
- (7) Vella, D.; Metcalfe, P. D.; Whittaker, R. J. *J. Fluid Mech.* **2006**, *549*, 215–224.
- (8) Gaudet, S. *Phys. Fluids* **1998**, *10*, 2489–2499.

length translating at constant speed in the bulk. If we assume that the form of the flow in the fluid is not changed substantially from this, we may write

$$\varphi = \dot{H}_0(\xi + R^2/\xi) \cos \psi \quad (1)$$

where the (ξ, ψ) coordinate system is a two-dimensional polar coordinate system with origin at the cylinder's center (the angle ψ being measured in the same sense as β in Figure 1), R is the (nondimensional) radius of the cylinder, and dots denote time derivatives. In reality, the velocity potential of the flow will be modified by the presence of the interface and so will not take the simple form assumed in (1). However, since the cylinder starts close to half immersed in the fluid, we expect these corrections to be small initially and make use of (1) in what follows.

Since the cylinder is accelerating, the reference frame in which (1) was calculated is not an inertial frame. The unsteady version of Bernoulli's theorem therefore takes the form¹⁰

$$F(T) = P - P_a + H + \frac{\partial \varphi}{\partial T} + \frac{1}{2} |\nabla \varphi|^2 - R \cos \psi \ddot{H}_0 \quad (2)$$

where P_a is atmospheric pressure. The value of the function $F(T)$ is determined by requiring that at the contact line, $\xi = R$ and $\psi = \beta$, the pressure is hydrostatic (i.e., $P - P_a = -H$). With this assumption, we may immediately write

$$F(T) = 2\dot{H}_0^2 \sin^2 \beta + R\ddot{H}_0 \cos \beta$$

and the pressure beneath the cylinder is given by

$$P(R, \psi) = P_a - H + R\ddot{H}_0(\cos \beta - \cos \psi) + 2\dot{H}_0^2(\sin^2 \beta - \sin^2 \psi) \quad (3)$$

This then allows us to calculate the vertical component of the pressure force acting on the cylinder as

$$F_p = \int_{-\beta}^{\beta} (P - P_a) \cos \psi R d\psi$$

$$= -2H_0 R \sin \beta + R^2(\beta + \cos \beta \sin \beta) + R^2(\cos \beta \sin \beta - \beta)\ddot{H}_0 + \frac{8}{3}\dot{H}_0^2 \sin^3 \beta \quad (4)$$

Upon letting $\mathcal{D} = \rho_s/\rho$ be the ratio of solid to liquid densities, we may then write Newton's second law for the height of the cylinder's center of mass above the free surface, H_0 , in the form

$$\mathcal{D}\pi R^2 \ddot{H}_0 = F_p - \pi R^2 \mathcal{D} + 2 \sin \phi \quad (5)$$

The second term on the right-hand side of (5) represents the weight of the cylinder acting downward, whereas the third term arises from the vertical component of the surface tension, which acts at an angle ϕ to the horizontal. Substituting (4) into (5) gives a simple second-order ordinary differential equation for $H_0(T)$ once the values of ϕ and β are determined.

A relationship between ϕ and β closes the system but must in general be determined by the numerical solution of the appropriate free-boundary problem. Here we instead investigate two much simplified closure models based on observations from experiments. The first observation is that the measured value of the contact angle θ is approximately constant over the course of the experiment (see Figure 3a), although its dynamic value θ_d

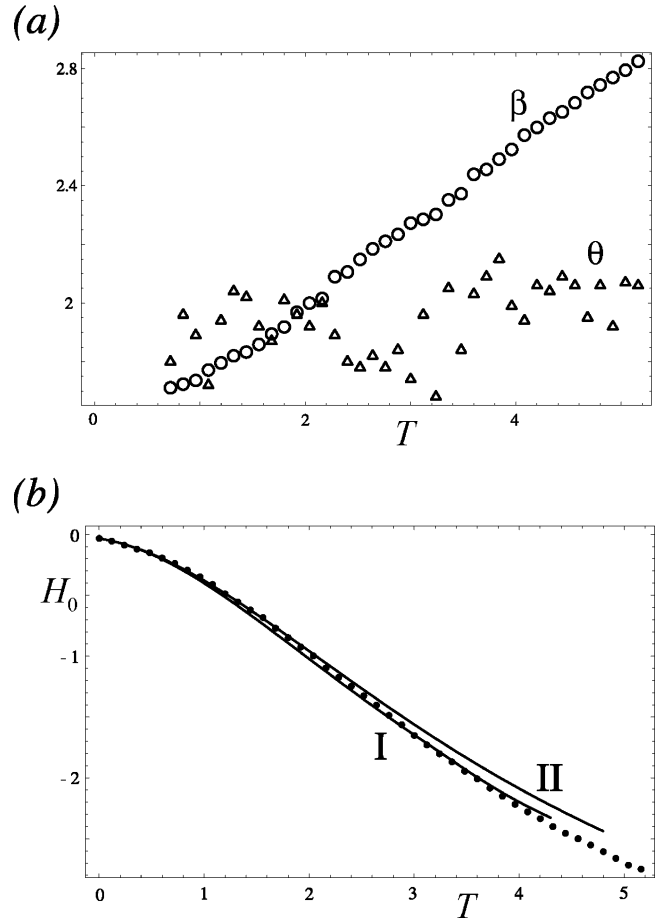


Figure 3. Experimental results for a cylinder with $\mathcal{D} = 1.92$ and $R = 0.93$. (a) Measurements of the contact angle, θ , and the angular position of the contact line, β , measured in radians as functions of nondimensional time, T . (b) Comparison of two closure models with experimental data (points). In I, ϕ is determined using the Laplace–Young equation, which in turn determines β . In II, we use the empirically determined linear dependence of β on T and infer from this the value of ϕ from the geometrical condition $\phi = \theta + \beta - \pi$.

$= 111^\circ$ is different from the equilibrium value. This is consistent with the observations of Ablett¹¹ for a hydrophobic solid at an air–water interface and so is used in both of the models described below.

The second observation is that the angular position of the contact line, β , increases approximately linearly in time, so that the contact line slips past the cylinder at a constant velocity, Figure 3a. This suggests that the system may be closed in an ad hoc manner by determining an empirical linear relationship for $\beta(T)$ and deducing ϕ from the geometrical relationship $\phi = \theta_d + \beta(T) - \pi$. Alternatively, this closure may be obtained by assuming that the first integral of the Laplace–Young equation¹²

$$\sin \phi = -H^*(1 - H^{*2}/4)^{1/2} \quad (6)$$

where $H^* = H_0 - R \cos \beta_0$ is the height of the contact line, holds. Since the Laplace–Young equation¹² arises from the consideration of hydrostatic equilibrium, eq 6 is entirely consistent with the assumption of a hydrostatic meniscus of our model. We expect this assumption to be valid at short times, as already discussed, and so expect (6) to also be valid at short times.

Both of the approximate closure schemes lead to an evolution of H_0 in reasonable quantitative agreement with experimental

(10) Paterson, A. R. *A First Course in Fluid Dynamics*; Cambridge University Press: Cambridge, U.K., 1983.

(11) Ablett, R. *Philos. Mag.* **1923**, *46*, 244–256.

(12) Mansfield, E. H.; Sepangi, H. R.; Eastwood, E. A. *Philos. Trans. R. Soc. London A* **1997**, *355*, 869–919.

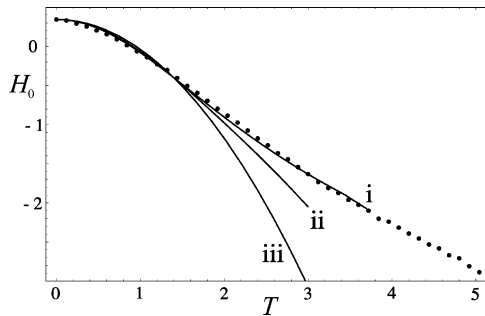


Figure 4. Experimental measurements of the cylinder's center position as a function of nondimensional time (points) compared to three variants of the theoretical model for a cylinder with $\mathcal{D} = 3.13$ and $R = 0.56$. Full model of sinking (i) and the full model without any retardation due to surface tension (ii). Line (iii) shows the free fall of a fully immersed cylinder, given by (7).

measurements, as shown in Figure 3b. We stress that there are no fitting parameters in our model, with the initial velocity of the cylinder determined from the first three frames of the experimental movie.

Experiments were conducted using hollow glass cylinders with length, L , much greater than their radius (typically, $L > 30R$) to ensure that three-dimensional effects were minimized. The surface of the cylinders was coated with a commercial nitrocellulose lacquer to increase the cylinders' equilibrium contact angle to $\theta = 72^\circ$. When metal wires were inserted into the hollow cavity of the cylinder and the cavity sealed with a semi-flexible polymer, the density of the cylinders could be varied simply ensuring that they were too dense to float unsupported at an air–water interface. The prepared cylinders were then placed (using a gripper) at the interface between air and water contained in a transparent tank. To eliminate the possibility of an interaction with the wall, the cylinder was placed at least 15 cm away from the walls of the tank.

Upon release, the cylinder sank rapidly since the vertical force contribution from the surface deformation was not sufficient to balance its weight. This sinking motion was observed through the side of the transparent tank via a high-speed CCD camera recording images at a rate of 500 s^{-1} giving rise to the typical time series illustrated in Figure 2. Image analysis software (Microsoft Photoeditor) was then used to determine the height of the cylinder center above the undeformed surface, H_0 , as a function of time, T , after release. Typical results are shown in Figure 4 for a smaller cylinder than was used in Figure 3b.

Along with the experimental results plotted in Figure 4 are a series of solid lines showing the theoretical predictions for the cylinder position produced with variants of model I, which was presented earlier. Again the first three data points were used to

determine the initial cylinder velocity, ensuring that our model has no free parameters. The simplest of the three variants of model I is the free-fall of the cylinder (with added mass) in the bulk liquid.¹⁰ This leads to the prediction

$$H_0(T) = H_0(0) + \dot{H}_0(0)T - \frac{\mathcal{D}}{2(\mathcal{D} + 1)}T^2 \quad (7)$$

which is illustrated by line iii in Figure 4. The solution of a more refined model, based on (5) but without the third term of the right-hand side associated with surface tension, is shown by line ii in Figure 4. Finally, the full solution of (5) including surface tension is shown by line i.

These show that a very simple model of the sinking process produces qualitatively similar results to those obtained from experiments. However, upon including modified hydrodynamic terms this agreement is substantially improved. Although the effect of surface tension is fairly small in our experiments, the model including surface tension agrees well with experiments right up to the time when a hydrostatic meniscus cannot join to the cylinder.

All of these models and experimental results indicate that the sinking occurs over a time scale $T \sim \mathcal{O}(1)$, which is modified by multiplicative prefactors that our analysis is able to predict with a reasonable accuracy. Physically this time scale is the time taken for the object to free-fall through the capillary length demonstrating that it is this falling motion that dominates the sinking process.

That the model presented here is able to capture the essential features of the motion quantitatively is somewhat surprising since we have paid only minimal attention to the meniscus profile and thus to the precise value of the force that is produced by surface tension. This success is partially due to the fact that the experiments presented here had a Bond number, $B \equiv R^2$, in the range (0.1, 1) so that the effects of surface tension do not completely dominate hydrostatic pressure (as evidenced by the similarity between the results with and without surface tension). However, a similar approach that simplifies the contribution from surface tension has been successfully used to describe the oscillations of a floating particle in a viscous fluid obtained via full numerical simulations.¹³ The success of our reduced model in describing the results of experiments suggests that similar approaches may be made to related problems, if only as a first step to understanding the essential physics.

Acknowledgment. D.V. is supported by the EPSRC. H.Y.K. gratefully acknowledges support from the faculty startup fund of Seoul National University.

LA0533260

(13) Singh, P.; Joseph, D. D. *J. Fluid Mech.* **2005**, *530*, 31–80.